Journal of Mathematical Modeling
Vol. 7, No. 1, 2019, pp. 85-106

JMM

Solving a time-fractional inverse heat conduction problem with an unknown nonlinear boundary condition

Afshin Babaei *

Department of Mathematics, University of Mazandaran, Babolsar, Iran
email: babaei@umz.ac.ir

Abstract. In this paper, we consider a time-fractional inverse heat conduction problem with an unknown function in the nonlinear boundary condition. First, ill-posedness of this problem is shown. Thus, we will apply the mollification regularization method with Gauss kernel to regularize the problem, then the space marching finite difference method is considered to solve numerically the mollified problem. The generalized cross-validation choice rule is used to find a suitable regularization parameter. The numerical scheme is completely described and the stability and convergence of the solutions are investigated. Finally, some numerical examples are presented to illustrate the validity and effectiveness of the proposed algorithm.

Keywords: Inverse problem, Caputo's fractional derivative, Ill-posedness, Mollification, Convergence analysis.
AMS Subject Classification: 65M32, 35R11, 35R30.

1 Introduction

In recent decades, fractional calculus and fractional differential equations have been used widely to model a range of phenomena in different fields of sciences, such as physics, chemistry, biology and engineering [3, 4, 9, 12, 18, 22, 26]. The main reason for this occurrence is the memory and hereditary properties of the fractional operators. Thus, fractional calculus has been

*Corresponding author.
Received: 9 November 2018 / Accepted: 29 December 2018.
DOI: 10.22124/jmm.2018.11656.1204

introduced as an efficient tool for modeling physical problems. For example, fractional models have been successfully used to describe anomalous difiusion processes such as contaminant transport in soil, oil flow in porous media, and groundwater flow [6, 23, 24]. The fractional-order dynamics of brainstem vestibulo-oculomotor neurons [1], dispersive transport of charge carriers in disordered nanostructured materials [25], the total fractional-order variation regularizer in non-rigid image registration in image inverse problems [31], fractional order HIV immune system with memory in the study of infectious diseases [5] are some other applications of fractional order systems.

In forward time-fractional heat conduction problems, the unknown temperature is derived from the known appropriate initial distribution and boundary conditions. However, in many practical situations some parameters such as initial or boundary functions, source term, a coefficient of the heat conduction equation or fractional order of the equation cannot be directly specified. Therefore, some inverse problems have to be solved to infer these unknown parameters indirectly from additional measured data. In recent ten years many authors worked on these types of problems. In [2, 15, 19, 20, 27, 28] authors considered some inverse problems related to the heat conduction equation to find the inaccessible boundary data through interior measurements. In [29] authors proposed an optimal regularization method to solve a fractional order backward heat conduction problem. In [11] and [17] some inverse source problems of the heat equation involving fractional derivative were investigated. Also, in [32] the optimal order of Caputo's fractional derivative for time-fractional heat conduction in a composite medium is estimated with Levenberg-Marquardt method. These inverse problems are generally ill-posed, namely, in present of noisy data, the solution of problems are not continuously dependent on the input data [10, 13]. Thus, the researchers combine their proposed algorithms with appropriate regularization methods to find stable numerical solutions. In this work, we investigate an inverse problem related to a time-fractional heat conduction equation with an unknown boundary function. Firstly, the problem is stabilized by using the mollification regularization technique. Afterwards, a numerical scheme based on the space marching finite difference method will be introduced to approximate the solution of the problem.

Bearing these ideas in mind, the manuscript is organized as follows. In Section 2, description of the inverse problem is considered and its ill-posedness is indicated. In Section 3, the mollification method is described and applied to the inverse problem in order to find a regularized problem.

Afterwards, the space marching algorithm for the numerical solution of the mollified problem is given. The stability and convergence of the proposed numerical scheme are studied in Section 4. Finally, some numerical test problems are investigated in Section 5.

2 Formulation of the problem

In this work, the one-dimensional time-fractional inverse heat conduction equation

$$D_t^{(\alpha)}u(x,t) = u_{xx}(x,t), \qquad 0 < x < 1, \quad 0 < t < 1, \tag{1}$$

with the initial condition

$$u(x,0) = u_0(x), \qquad 0 \le x \le 1, \tag{2}$$

and the boundary conditions

$$u_x(0,t) = \gamma(t), \qquad 0 \le t \le 1, \tag{3}$$

$$-u_x(1,t) = f(u(1,t)) + \eta(t), \qquad 0 \le t \le 1, \tag{4}$$

is considered, where $u_0(x) \in L^2([0,1])$ is the given initial temperature, $\eta(t)$ and $\gamma(t)$ are considered to be known continuous functions and $f(u)$ is the unknown boundary function. It is assumed that f is a Lipschitz continuous function and satisfies the compatibility condition $-u_0'(1) = f(u_0(1)) + \eta(0)$. In Eq. (1) $D_t^{(\alpha)}(.)$ is the Caputo time-fractional derivative of order $0 < \alpha < 1$ defined as [16]

$$D_t^{(\alpha)}\xi(t) = \frac{1}{\Gamma(1-\alpha)} \int_0^t \frac{\xi'(s)}{(t-s)^\alpha} ds, \qquad 0 \le t \le 1, \tag{5}$$

where ξ is a differentiable function and $\Gamma(.)$ is the Gamma function.

To determine the set of functions (u, f) in the problem (1)-(4) we need a additional condition. Here, the condition

$$u(0,t) = p(t), \qquad 0 \le t \le 1, \tag{6}$$

is used. This problem with $\eta(t) = 0$ has been considered in [21] and the existence and uniqueness of the solution for this inverse problem is proved by applying the fixed point theorem. In our numerical approach that follows, we will assume that the solution of the problem (1)-(6) is a sufficiently smooth function.

In practice, the input functions $u_0(x), \gamma(t), \eta(t)$ and $p(t)$ are not exact, but some perturbed versions of them are in hand. On the other hand, the problem (1)-(6) is ill-posed, i.e. small errors in the input functions can blow up in the solution. To show the ill-posedness of this problem, we solve it in the frequency domain. For this purpose, all the related functions are extended to the whole real line $\mathbb{R}$ by defining them to be zero for $(-\infty, 0) \cup (1, +\infty)$. Taking the Fourier transform of Eqs. (1), (3) and (6) with respect to t [18], we get

$$(i\omega)^{\alpha}\hat{u}(x,\omega) = \hat{u}_{xx}(x,\omega), \tag{7}$$

$$\hat{u}_x(0,\omega) = \hat{\gamma}(\omega), \tag{8}$$

$$\hat{u}(0,\omega) = \hat{p}(\omega), \tag{9}$$

where

$$(i\omega)^{\alpha} = |\omega|^{\alpha}\big(\cos\frac{\alpha\pi}{2} + isgn(\omega)\sin\frac{\alpha\pi}{2}\big),$$

and $sgn(\omega)$ is the sign function. The second-order ordinary differential equation (7) under the conditions (8) and (9) has the following solution:

$$\hat{u}(x,\omega) = \cosh\big((i\omega)^{\frac{\alpha}{2}}x\big)\hat{p}(\omega) + (i\omega)^{-\frac{\alpha}{2}}\sinh\big((i\omega)^{\frac{\alpha}{2}}x\big)\hat{\gamma}(\omega).$$

Now, suppose that the input data functions $u_0(x)$, $\gamma(t)$ and $\eta(t)$ be exact and we have only noisy data $p(t)$. Let the measured data $p^{\varepsilon}(t)$ satisfy $p^{\varepsilon}(t) = p(t) + \varepsilon(t)$, where $\varepsilon \in L^2(\mathbb{R})$ is the measured error. Hence, the solution to the problem (7)-(9) has the form

$$\hat{\vartheta}(x,\omega) = \hat{u}(x,\omega) + \cosh\big((i\omega)^{\frac{\alpha}{2}}x\big)\hat{\delta}(\omega). \tag{10}$$

Let the solution $\hat{u}(x,\omega)$ belongs to $L^2(\mathbb{R})$ with respect to ω. For a fixed value $0 < x < 1$, $\cosh\big(|\omega|^{\frac{\alpha}{2}}\cos\frac{\alpha\pi}{4}x\big)$ is unbounded as $\omega \to \infty$. Therefore, the exact input data function $\hat{p}(\omega)$ must decay rapidly. But, we have the noisy data $p^{\varepsilon}(t) \in L^2(\mathbb{R})$ and cannot expect the measurement data $\hat{p}^{\varepsilon}(\omega)$ to have the same decay in the frequency domain as the exact data $\hat{p}(\omega)$. Hence, in general, the solution $\hat{\vartheta}(x,\omega)$ will not belongs to $L^2(\mathbb{R})$. So, the numerical solution will be destroied by magnified high frequency components of the error ε. Thus, to solve the problem (1)-(4), we require a regualarization method. The mollification technique utilizes a convolution of the input data and a smooth function with a parameter, to filter the high-frequency components of the noisy data. Therefore, the problem becomes well-posed. This method is being widely used as regularization method in many ill-posed problems [7, 8, 13, 30]. The simplicity of implementation and capability in the presence of high noise levels are principal advantages of the mollification technique.

3 Numerical scheme

3.1 Mollification method

Let $\delta > 0$, $p > 0$, and

$$A_p = \Big(\int_{-p}^{p} exp(-s^2) ds \Big)^{-1}.$$

The δ-mollification of an integrable function is based on a convolution with the Gaussian kernel

$$\rho_{\delta,p}(t) = \begin{cases} A_p \delta^{-1} \exp(-\frac{t^2}{\delta^2}), & |t| \le p\delta, \\ 0, & |t| > p\delta. \end{cases}$$

The δ-mollifier $\rho_{\delta,p}$ is a non-negative function on space of infinitely differentiable functions in $(-p\delta, p\delta)$ and satisfying $\int_{-p\delta}^{p\delta} \rho_{\delta,p}(t)dt = 1$. Suppose $\zeta(t)$ is a locally integrable function in $\mathbb{R}$. The δ-mollification of $\zeta(t)$ is defined by the convolution

$$\mathcal{J}_\delta \zeta(t) = (\rho_\delta * \zeta)(t) = \int_{t-p\delta}^{t+p\delta} \rho_\delta(t-s)\zeta(s)ds,$$

where the p-dependency on the kernel has been dropped for simplicity of notation. The radius of mollification δ is determined automatically by the Generalized Cross Validation (GCV) ceriteria [13]. In order to define the mollification of a discrete function, let

$$K = \{t_j : j \in Z\},$$

and $\Delta t = \sup_{j \in Z}(t_{j+1} - t_j)$, satisfy

$$t_{j+1} - t_j > d > 0 \ , \quad j \in Z,$$

where Z is a set of integers, and d is a positive constant.

Let $G = \{\zeta(t_j) = \zeta_j : j \in Z\}$ be a discrete function defined on K. We set

$$s_j = \frac{1}{2}(t_j + t_{j+1}) \ , \quad j \in Z.$$

The discrete δ-mollification of G is defined as follows:

$$\mathcal{J}_\delta G(t) = \sum_{j=-\infty}^{\infty} \Big(\int_{s_{j-1}}^{s_j} \rho_\delta(t-s)ds \Big) \zeta_j,$$

where

$$\sum_{j=-\infty}^{\infty}\Big(\int_{s_{j-1}}^{s_j}\rho_\delta(t-s)ds\Big)=\int_{-p\delta}^{p\delta}\rho_\delta(s)ds=1.$$

We assume that instead of the function ζ, we know some noisy data function ζ^ε such that $\|\zeta-\zeta^\varepsilon\|_\infty\le\varepsilon$.

Theorem 1. *Let the functions ζ and ζ' are uniformly Lipschitz on $\mathbb{R}$. Also let $G=\{\zeta_j : j\in Z\}$ and $G^\varepsilon=\{\zeta_j^\varepsilon : j\in Z\}$ be the discrete version of ζ and ζ^ε, which are defined on K, satisfying $\|\zeta-\zeta^\varepsilon\|_\infty\le\varepsilon$ and $\|G-G^\varepsilon\|_\infty\le\varepsilon$. Then*
i) there exists a constant $\mathcal{C}$, independent of δ, such that

$$\|\mathcal{J}_\delta G-\zeta\|_\infty\le\mathcal{C}(\delta+\Delta t),\tag{11}$$

and

$$\|(\mathcal{J}_\delta G)'-\zeta'\|_\infty\le\mathcal{C}\Big(\delta+\frac{\varepsilon+\Delta t}{\delta}\Big).\tag{12}$$

ii) if $\|G-G^\varepsilon\|_\infty\le\varepsilon$, then

$$\|\mathcal{J}_\delta G-\mathcal{J}_\delta G^\varepsilon\|_\infty\le\varepsilon.\tag{13}$$

Also, there exists a constant $\mathcal{C}$, independent of δ, such that

$$\|(\mathcal{J}_\delta G)'-(\mathcal{J}_\delta G^\varepsilon)'\|_\infty\le\mathcal{C}\frac{\varepsilon}{\delta}.\tag{14}$$

Theorem 2. *Let a differentiation operator $\mathcal{D}_0^\delta$ be defined by the following rule:*

$$\mathcal{D}_0^\delta(G)=\mathcal{D}_0(\mathcal{J}_\delta G)(t)\Big|_K,$$

in which $\mathcal{D}_0$ is the centeral difference operator

$$\mathcal{D}_0\zeta(t)=\frac{\zeta(t+\Delta t)-\zeta(t-\Delta t)}{2\Delta t}.$$

Then

$$\|\mathcal{D}_0^\delta(G)\|_\infty\le\frac{4A_p}{\delta}\|G\|_\infty.$$

The proofs of these theorems can be found in the reference [13].

3.2 Mollified fractional derivative

The process of numerical fractional differentiation is well known to be an ill-posed problem, because a small error in measurement data can induce a large error in the approximate derivative. Suppose $\zeta^\varepsilon(t)$ is a perturbed version of the exact function $\zeta(t)$. To approximate $\mathcal{J}_\delta(D_t^{(\alpha)}\zeta^\varepsilon)$ on a uniform partition K of the unit interval, we follow the mollification technique proposed in [14].

Let $\mathcal{D}_+$ be forward finite difference operator. The discrete computed solution $(D_t^{(\alpha)}G^\varepsilon)_\delta$ of the mollified function $\mathcal{J}_\delta(D_t^{(\alpha)}\zeta^\varepsilon)$ in the grid points, will be as

$$\begin{aligned}
\Big(D^{(\alpha)}G^\varepsilon\Big)_\delta(t_1) &= \mathcal{D}_+(\mathcal{J}_\delta G^\varepsilon)(t_1)W_1\\
\Big(D^{(\alpha)}G^\varepsilon\Big)_\delta(t_2) &= \mathcal{D}_+(\mathcal{J}_\delta G^\varepsilon)(t_1)W_2 + \mathcal{D}_+(\mathcal{J}_\delta G^\varepsilon)(t_2)W_1,\\
\Big(D^{(\alpha)}G^\varepsilon\Big)_\delta(t_j) &= \mathcal{D}_+(\mathcal{J}_\delta G^\varepsilon)(t_1)W_j\\
&\quad + \sum_{i=2}^{j-1}\mathcal{D}_0(\mathcal{J}_\delta G^\varepsilon)(t_i)W_{j-i+1} + \mathcal{D}_+(\mathcal{J}_\delta G^\varepsilon)(t_j)W_1,
\end{aligned} \tag{15}$$

where $j = 3, 4, \ldots, n$ and the weights W_j are as follows:

$$\begin{aligned}
W_1 &= \frac{1}{\Gamma(2-\alpha)}\Big(\frac{\Delta t}{2}\Big)^{1-\alpha},\\
W_i &= \frac{1}{\Gamma(2-\alpha)}\Big[\Big((2i+1)\frac{\Delta t}{2}\Big)^{1-\alpha} - \Big((2i-1)\frac{\Delta t}{2}\Big)^{1-\alpha}\Big],
\end{aligned}$$

where $i = 2, 3, \ldots, j-1$, and

$$W_j = \frac{1}{\Gamma(2-\alpha)}\Big[j\Delta t - \Big[\Big(j-\frac{1}{2}\Big)\Delta t\Big]^{1-\alpha}\Big].$$

Theorem 3. *Let the functions ζ' and ζ^ε are uniformly Lipschitz on $\mathbb{R}$ as $\|\zeta - \zeta^\varepsilon\|_\infty \le \varepsilon$. Also, suppose G and G^ε, the discrete versions of ζ and ζ^ε, satisfy $\|G - G^\varepsilon\|_\infty \le \varepsilon$. Then*

$$\Big\|(D_t^{(\alpha)}G^\varepsilon)_\delta - D_t^{(\alpha)}\zeta\Big\|_\infty \le \frac{\mathcal{C}}{\Gamma(2-\alpha)}\Big(\delta + \frac{\varepsilon}{\delta} + \Delta t\Big),$$

where $\mathcal{C}$ is a constant independent of δ.

Proof. Refer to [14]. □

3.3 The δ-mollified space marching algorithm

Suppose $\upsilon = \mathcal{J}_\delta u$ is the mollified version of u. The regularized problem is formulated as follows

$$\begin{array}{ll} D_t^{(\alpha)}\upsilon(x,t) = \upsilon_{xx}(x,t), & 0 < x < 1,\ 0 < t < 1, \\ \upsilon(x,0) = \mathcal{J}_\delta u_0^\varepsilon(x), & 0 \le x \le 1, \\ \upsilon(0,t) = \mathcal{J}_{\delta_0} p^\varepsilon(t), & 0 \le t \le 1, \\ \upsilon_x(0,t) = \mathcal{J}_{\delta_0'} g^\varepsilon(t), & 0 \le t \le 1, \end{array} \tag{16}$$

where δ, δ_0 and $\delta_0^{'}$ are the radii of mollification, and will be chosen using the GCV criteria. After solving (16), the mollified function $\mathcal{F}(\upsilon)$ is obtained from

$$-\upsilon_x(1,t) = \mathcal{F}(\upsilon(1,t)) + \mathcal{J}_{\delta''}\eta^\varepsilon(t), \quad 0 \le t \le 1, \tag{17}$$

Let M and N be two positive integers. We consider a uniform grid in the unit interval $I = [0,1] \times [0,1]$ as

$$\{(x_i = ih, t_n = nk)\ ,\ \ i = 0,1,\ldots,M;\ \ n = 0,1,\ldots,N\},$$

in which $Mh = 1$ and $Nk = 1$. Let the value of $\upsilon(x,t)$ at (x_i,t_n) is indicated by R_i^n. In addition, suppose

$$W_i^n = \upsilon_x(ih,nk)\ ,\ \ Q_i^n = D_t^{(\alpha)}\upsilon(ih,nk)\ ,\ \ \eta_n = \mathcal{J}_{\delta''}\eta^\varepsilon(nk).$$

Let

$$R_0^n = \mathcal{J}_{\delta_0} p^\varepsilon(nk),\ \ W_0^n = \mathcal{J}_{\delta_0'} g^\varepsilon(nk),\ \ Q_0^n = D_t^{(\alpha)}(\mathcal{J}_{\delta_0} p^\varepsilon(nk)),\ \ n \in \{1,\ldots,N\},$$

and

$$R_i^0 = \mathcal{J}_\delta u_0^\varepsilon(ih),\ \ i \in \{0,1,\ldots,M\}.$$

We approximate the partial differential equation in system (16) by the finite difference schemes

$$R_{i+1}^n = R_i^n + hW_i^n, \tag{18}$$

$$W_{i+1}^n = W_i^n + hQ_i^n, \tag{19}$$

$$Q_{i+1}^n = D_t^{(\alpha)}(\mathcal{J}_{\delta_{i+1}} R_{i+1}^n), \tag{20}$$

where $i = 0,\ldots,M-1$ and $n = 1,\ldots,N$. To approximate $D_t^{(\alpha)}(\mathcal{J}_{\delta_i} R_i^n)$, the quadrature formula (15) will be used. After applying these schemes, the values of $u(x,t)$ and $u_x(x,t)$ are calculated on the boundary $x = 1$. By substituting R_M^n and W_M^n in equation (17), we get

$$-W_M^n = \mathcal{F}(R_M^n) + \eta_n. \tag{21}$$

Finally the unknown function $\mathcal{F}$ is reconstructed by interpolating these values.

4 Stability and convergence analysis

Suppose the discrete function $G = \{\zeta_j = \zeta(t_j) : j \in Z\}$ is defined on K. After applying Theorem 2, we have

$$|D_t^{(\alpha)} \mathcal{J}_\delta G(t)| = \Big|\frac{1}{\Gamma(1-\alpha)} \int_0^t \frac{(\mathcal{J}_\delta G(s))'}{(t-s)^\alpha} ds\Big| = \Big|\frac{1}{\Gamma(1-\alpha)} \int_0^t \frac{\mathcal{D}_0(\mathcal{J}_\delta G(s))}{(t-s)^\alpha} ds\Big|$$
$$\leq \frac{1}{\Gamma(1-\alpha)} \int_0^t \frac{4A_p\|G\|_\infty}{\delta|(t-s)^\alpha|} ds = \frac{4A_p\|G\|_\infty t^{1-\alpha}}{\delta\Gamma(2-\alpha)}. \tag{22}$$

Theorem 4. *Suppose $|R_i|, W_i|, |Q_i|$ are maximum values of $|R_i^n|, |W_i^n|, |Q_i^n|$, where $n \in \{0, 1, \ldots, N\}$. For the marching scheme, there exists a constant θ, such that*

$$\max\{|R_M|, |W_M|, |Q_M|\} \leq \theta \max\{|R_0|, |W_0|, |Q_0|\}.$$

Proof. By using (18) and (19), we have

$$|R_{i+1}^n| \leq (1+h) \max\{|R_i^n|, |W_i^n|\}, \tag{23}$$

$$|W_{i+1}^n| \leq (1+h) \max\{|W_i^n|, |Q_i^n|\}. \tag{24}$$

Let $\delta' = \min_i\{\delta_i\}$, from (20), (22) and (23), we have

$$|Q_{i+1}^n| \leq \frac{4A_p(nk)^{1-\alpha}(1+h)}{\delta'\Gamma(2-\alpha)} \max\{|R_i^n|, |W_i^n|\}. \tag{25}$$

Let

$$\hat{\mathcal{C}} = \max\Big\{1, \frac{4A_p(nk)^{1-\alpha}}{\delta'\Gamma(2-\alpha)}\Big\},$$

from (23)-(25), we obtain

$$\max\{|R_{i+1}|, |W_{i+1}|, |Q_{i+1}|\} \leq (\hat{\mathcal{C}} + \hat{\mathcal{C}}h) \max\{|R_i|, |W_i|, |Q_i|\}. \tag{26}$$

By iterating (26), M times, we get

$$\begin{aligned}\max\{|R_M|, |W_M|, |Q_M|\} &\leq (\hat{\mathcal{C}} + \hat{\mathcal{C}}h) \max\{|R_{M-1}|, |W_{M-1}|, |Q_{M-1}|\} \\ &\leq (\hat{\mathcal{C}} + \hat{\mathcal{C}}h)^2 \max\{|R_{M-2}|, |W_{M-2}|, |Q_{M-2}|\} \\ &\leq \cdots \leq (\hat{\mathcal{C}} + \hat{\mathcal{C}}h)^M \max\{|R_0|, |W_0|, |Q_0|\},\end{aligned}$$

which implies

$$\max\{|R_M|, |W_M|, |Q_M|\} \leq \hat{\mathcal{C}}^M \exp(1) \max\{|R_0|, |W_0|, |Q_0|\}.$$

Letting $\theta = \hat{\mathcal{C}}^M \exp(1)$, completes the proof of this statement. □

Remark 1. *For the boundary function f, there exists a constant Φ, such that*

$$\max\{|\mathcal{F}(R_M)|\} \leq \Phi \max\{|R_0|, |W_0|, |Q_0|, |\eta|\}.$$

Proof. By using (21), we have

$$|\mathcal{F}(R_M^n)| \leq \max|W_M^n| + \max|\eta_n|,$$

and from Theorem 4, we have

$$\max|\mathcal{F}(R_M)| \leq \theta \max\{|R_0|, |W_0|, |Q_0|\} + \max|\eta_n|.$$

Letting $\Phi = \max\{1, \theta\}$, we obtain

$$\max\{|\mathcal{F}(R_M)|\} \leq \Phi \max\{|R_0|, |W_0|, |Q_0|, |\eta|\}.$$

□

Theorem 5. *For the marching schemes, when ε, h and k tend towards 0, by choosing $\delta' = \delta'(\varepsilon)$, the discrete mollified solution converges to the mollified exact solution.*

Proof. Suppose $i \in \{0, 1, ..., M\}$ and $n \in \{0, 1, ..., N\}$. First, we define the discrete error functions $\Delta R_i^n = R_i^n - \upsilon(ih, nk)$ and $\Delta W_i^n = W_i^n - \upsilon(ih, nk)$. By applying Theorem 1, we have

$$\begin{aligned}
|Q_i^n - D_t^{(\alpha)}\upsilon(ih, nk)| &= |D_t^{(\alpha)}\mathcal{J}_\delta u^\varepsilon(ih, nk) - D_t^{(\alpha)}\mathcal{J}_\delta u(ih, nk) + O(k)| \\
&= |D_t^{(\alpha)}(\mathcal{J}_\delta u^\varepsilon(ih, nk) - \mathcal{J}_\delta u(ih, nk)) + O(k)| \\
&\leq \frac{1}{\Gamma(1-\alpha)} \int_0^{nk} \frac{\mathcal{C}\varepsilon}{\delta(nk-s)^\alpha} ds + O(k) \\
&= \frac{\mathcal{C}\varepsilon(nk)^{1-\alpha}}{\delta\Gamma(2-\alpha)} + O(k) \\
&\leq \frac{\mathcal{C}\varepsilon}{\delta\Gamma(2-\alpha)} + O(k) \\
&= \mathcal{C}_\alpha \frac{\varepsilon}{\delta} + O(k),
\end{aligned}$$

where $\mathcal{C}_\alpha = \frac{\mathcal{C}}{\Gamma(2-\alpha)}$.

Expanding the mollified solution $\upsilon(x, t)$ by the Taylor series, we obtain

$$\upsilon((i+1)h, nk) = \upsilon(ih, nk) + h\upsilon_x(ih, nk) + O(h^2), \tag{27}$$

$$\upsilon_x((i+1)h, nk) = \upsilon_x(ih, nk) + hD_t^{(\alpha)}\upsilon(ih, nk) + O(h^2). \tag{28}$$

From (18) and (27), we have

$$\begin{aligned}\Delta R_{i+1}^n &= R_{i+1}^n - \upsilon((i+1)h, nk)\\ &= R_i^n + hW_i^n - \upsilon((i+1)h, nk)\\ &= R_i^n + hW_i^n - \upsilon(ih, nk) - h\upsilon_x(ih, nk) + O(h^2)\\ &= \Delta R_i^n + h\Delta W_i^n + O(h^2),\end{aligned} \tag{29}$$

and by using (19) and (28), we have

$$\begin{aligned}\Delta W_{i+1}^n &= W_{i+1}^n - \upsilon_x((i+1)h, nk)\\ &= W_i^n + hQ_i^n - \upsilon_x((i+1)h, nk)\\ &= W_i^n + hQ_i^n - \upsilon_x(ih, nk) - hD_t^{(\alpha)}\upsilon(ih, nk) + O(h^2)\\ &= \Delta W_i^n + h\mathcal{C}_\alpha\frac{\varepsilon}{\delta} + O(hk) + O(h^2).\end{aligned} \tag{30}$$

Let $|\Delta R_i| = \max\limits_{0\le n\le N}|\Delta R_i^n|$ and $|\Delta W_i| = \max\limits_{0\le n\le N}|\Delta W_i^n|$. Thus, from (29) and (30), we obtain

$$\begin{aligned}|\Delta R_{i+1}^n| &\le |\Delta R_i^n| + h|\Delta W_i^n| + O(h^2)\\ &\le \max_{0\le n\le N}|\Delta R_i^n| + h\max_{0\le n\le N}|\Delta W_i^n| + O(h^2)\\ &= |\Delta R_i| + h|\Delta W_i| + O(h^2),\end{aligned}$$

and

$$\begin{aligned}|\Delta W_{i+1}^n| &\le |\Delta W_i^n| + h\mathcal{C}_\alpha\frac{\varepsilon}{\delta} + O(hk) + O(h^2)\\ &\le \max_{0\le n\le N}|\Delta W_i^n| + h\mathcal{C}_\alpha\frac{\varepsilon}{\delta} + O(hk) + O(h^2)\\ &= |\Delta W_i| + h\mathcal{C}_\alpha\frac{\varepsilon}{\delta} + O(hk) + O(h^2).\end{aligned}$$

Hence

$$\begin{aligned}|\Delta R_{i+1}| &= \max_{0\le n\le N}|\Delta R_{i+1}^n| \le |\Delta R_i| + h|\Delta W_i| + O(h^2),\\ &\le (1+h)\max\{|\Delta R_i|, |\Delta W_i|\} + O(h^2),\\ |\Delta W_{i+1}| &= \max_{0\le n\le N}|\Delta W_{i+1}^n| \le |\Delta W_i| + h\mathcal{C}_\alpha\frac{\varepsilon}{\delta} + O(hk) + O(h^2),\\ &\le \max\{|\Delta W_i|\} + h\mathcal{C}_\alpha\frac{\varepsilon}{\delta} + O(hk) + O(h^2).\end{aligned}$$

Then, we have

$$\max\{|\Delta R_{i+1}|, |\Delta W_{i+1}|\} \le (1+h)\max\{|\Delta W_i|, |\Delta R_i|\} + \Lambda, \tag{31}$$

where $\Lambda = h\mathcal{C}_\alpha \frac{\varepsilon}{\delta} + O(hk) + O(h^2)$. Now, let $\Delta_i = \max\{|\Delta W_i|, |\Delta R_i|\}$. From (31), we have

$$\Delta_{i+1} \leq (1+h)\Delta_i + \Lambda, \tag{32}$$

and

$$\begin{aligned} \Delta_M &\leq (1+h)\Delta_{M-1} + \Lambda \leq (1+h)^2\Delta_{M-2} + (1+h)\Lambda + \Lambda \\ &\leq \cdots \leq (1+h)^M\Delta_0 + \tau\Lambda, \end{aligned} \tag{33}$$

where $\tau = \sum_{i=0}^{M-1} (1+h)^i$. Now by using Theorem 1, for $n \in \{0, 1, \ldots, N\}$, there exists constant $\mathcal{C}_n$ and $\mathcal{D}_n$, such that

$$\begin{aligned} |\Delta R_0^n| &= |R_0^n - \upsilon(0, nk)| \leq \mathcal{C}_n(\delta_0 + k), \\ |\Delta W_0^n| &= |W_0^n - \upsilon_x(0, nk)| \leq \mathcal{D}_n(\delta_0^{'} + k), \end{aligned}$$

let $\delta' = \max\{\delta_0, \delta_0'\}$ and $\mathcal{C}' = \max\{\mathcal{C}_n, \mathcal{D}_n |\ n = 0, \ldots, N\}$, then we have

$$\Delta_0 = \max\{|\Delta R_0^n|, |\Delta W_0^n|\} \leq \mathcal{C}'(\delta' + k),$$

and

$$\Delta_M \leq exp(1)\mathcal{C}'(\delta' + k) + \tau\Lambda. \tag{34}$$

Thus when ε, h and k tend towards 0, by choosing $\delta' = \delta^{'}(\varepsilon)$, Δ_M will tend to 0. It completes the proof. □

Remark 2. *For the marching schemes, when ε, h and k tend towards 0, the discrete mollified boundary function $\mathcal{F}$ converges to the mollified exact boundary function f.*

Proof. Suppose $\Delta\mathcal{F}_n = \mathcal{F}(\upsilon(1, nk)) - \mathcal{F}(R_M^n)$. By using (17) and (21), we have

$$\begin{aligned} \Delta\mathcal{F}_n &= (-\upsilon(1, nk) - \mathcal{J}_{\delta''}\eta^\varepsilon(nk)) - (-W_M^n - \eta_n) \\ &= (W_M^n - \upsilon(1, nk)) + (\eta_n - \mathcal{J}_{\delta''}\eta^\varepsilon(nk)) \\ &= \Delta W_M^n + (\eta_n - \mathcal{J}_{\delta''}\eta^\varepsilon(nk)), \end{aligned}$$

by applying Theorem 1, we have

$$|\Delta\mathcal{F}_n| \leq |\Delta W_M^n| + |(\eta_n - \mathcal{J}_{\delta''}\eta^\varepsilon(nk))| \leq \Delta_M + \varepsilon,$$

consequently by using (34), we have

$$|\Delta\mathcal{F}_n| \leq \exp(1)\mathcal{C}'(\delta' + k) + \tau\Lambda + \varepsilon.$$

This implies that when ε, h and k tend to zero,$|\Delta\mathcal{F}_n|$ tend towards zero too. It completes the proof. □

5 Numerical Implementation

Suppose the number of space and time divisions are M and N. Let $h = \frac{1}{M}$ and $k = \frac{1}{N}$ and ε be the maximum level of noises in the data. We use the following formula to generate the noisy data

$$s_n^{\varepsilon} = s(t_n) + \varepsilon_n, \qquad n = 0, \ldots, N,$$

where $s(t_n)$ is the exact data and ε_n is a Gaussian random variable with variance $\sigma^2 = \varepsilon^2$ [13].

The temperature and heat flux errors are measured by the relative weighted l_2-norm defined as

$$\sigma_N(u) = \frac{\left(\frac{1}{N+1}\sum_{n=0}^{N} |R_M^n - u(1,nk)|^2\right)^{\frac{1}{2}}}{\left(\frac{1}{N+1}\sum_{n=0}^{N} |u(1,nk)|^2\right)^{\frac{1}{2}}},$$

and the boundary function $f(u)$ errors are measured by

$$\sigma_N(f) = \frac{\left(\frac{1}{N+1}\sum_{n=0}^{N} |\mathcal{F}(R_M^n) - f(u(1,nk))|^2\right)^{\frac{1}{2}}}{\left(\frac{1}{N+1}\sum_{n=0}^{N} |f(u(1,nk))|^2\right)^{\frac{1}{2}}}.$$

Example 1. Consider the following problem:

$$\begin{cases} D_t^{(\alpha)} u(x,t) = u_{xx}(x,t), & (x,t) \in [0,1] \times [0,1], \\ u(x,0) = u_0(x) = \begin{cases} x, & x \in [0, \frac{1}{2}], \\ 1-x, & x \in [\frac{1}{2}, 1], \end{cases} \\ u(0,t) = 0, & t \in [0,1], \\ u_x(0,t) = \sum\limits_{n=1}^{\infty} n d_n E_\alpha(-n^2 t^\alpha), & t \in [0,1], \end{cases}$$

where

$$d_n = \frac{2}{\pi}\int_0^{\pi} u_0(x)\sin(nx)dx = \frac{2(1+(-1)^{n+1})}{\pi n^2}\Big(\sin(\frac{n\pi}{2}) - \frac{n\pi}{2}\cos(\frac{n\pi}{2})\Big),$$

for $n = 1, 2, \ldots$. Also, suppose

$$\eta(t) = -1 - \sum_{n=1}^{\infty} n d_n E_\alpha(-n^2 t^\alpha)\cos(n) - 2\ sin\Big(\sum_{n=1}^{\infty} d_n E_\alpha(-n^2 t^\alpha)\sin(n)\Big).$$

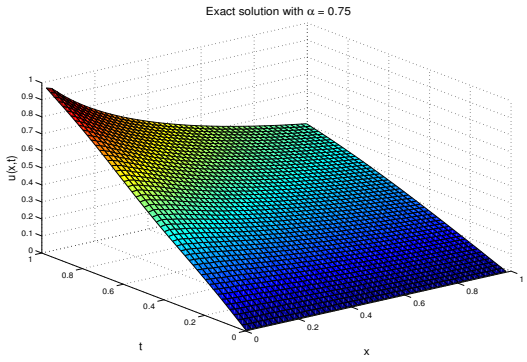

Figure 1: The exact solution of $u(x,t)$ for Example 1 when $\alpha = 0.75$.

The exact solution is

$$u(x,t) = \sum_{n=1}^{\infty} d_n E_\alpha(-n^2 t^\alpha) \sin(nx),$$

where $E_\alpha(.)$ is the Mittag-Leffler function and

$$f(u) = 1 + 2\sin(4\pi u).$$

After adding noise to the data, to generate the noisy functions $u^\varepsilon(0,t)$, $u_x^\varepsilon(0,t)$ and $u^\varepsilon(x,0)$, the mollified problem (16) is solved with the various values of the parameters h, k and the time fractional order α.

Figure 1 shows the exact solution of $u(x,t)$ and Figure 2 and Figure 3 show the numerical approximation and absolute error of $u(x,t)$ when $\alpha = 0.75$, $M = 150, N = 150$, $\varepsilon = 0.01$ and $\varepsilon = 0.05$.

Table 1 displays the errors of the approximated values of temperature and heat flux at the boundary $x = 1$ and $f(u)$. Furthermore, Figure 4 shows the numerical approximations of $f(u)$ with regularization and without regularization when $M = 100, N = 128$, $\alpha = 0.8$ and $\varepsilon = 0.1$. Also, Figure 5 shows the exact and numerical approximations to $f(u)$ for several values of $\varepsilon = 0.001, 0.01, 0.05, 0.1$, when $M = 50, N = 128$, $\alpha = 0.5$. Finally, Figure 6 indicates the absolute error of numerical approximations for $f(u)$.

Example 2. Consider the problem (1)-(4) with $u_0(x) = e^{-x}$, $\gamma(t) = -E_\alpha(t^\alpha)$ and $p(t) = E_\alpha(t^\alpha)$. The exact solution of this problem is

$$u(x,t) = E_\alpha(t^\alpha)e^{-x},$$

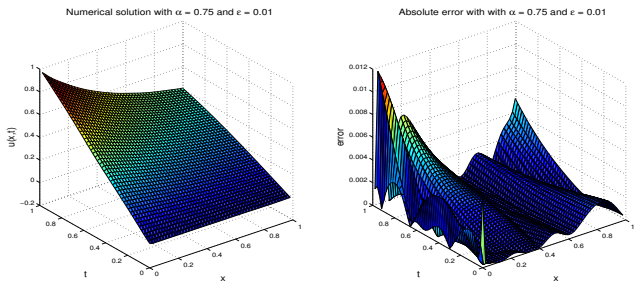

Figure 2: The numerical solution and absolute error of $u(x,t)$ for Example 1 when $\alpha = 0.75$ and $\varepsilon = 0.01$.

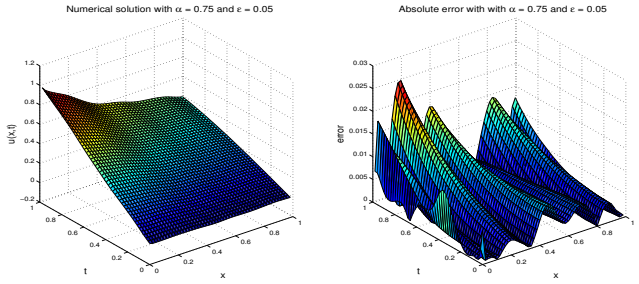

Figure 3: The numerical solution and absolute error of $u(x,t)$ for Example 1 when $\alpha = 0.75$ and $\varepsilon = 0.05$.

where $E_\alpha(.)$ is the Mittag-Leffler function and $f(u) = u^3 - \alpha u + 1$.

Figure 7, Figure 8 and Figure 9 show the exact and numerical solutions of $u(x,t)$ when $M = 150, N = 150$, $\alpha = 0.25, 0.5, 0.75$ and $\varepsilon = 0.05$.

Table 2 indicates the errors of the approximated values of temperature and heat flux at the boundary $x = 1$ and $f(u)$. Also, Figure 10 shows the exact and numerical solutions (left) and absolute error (rigth) of $f(u)$ when $N = 50$, $\alpha = 0.5$, $\varepsilon = 0.01$ and $M = 50, 100, 150$.

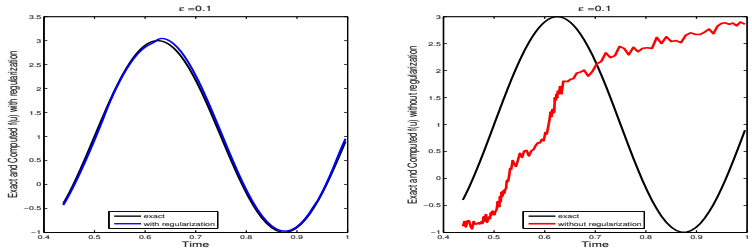

Figure 4: The numerical approximations of $f(u)$ with regularization and without regularization in Example 1 when $\alpha = 0.8$ and $\varepsilon = 0.1$.

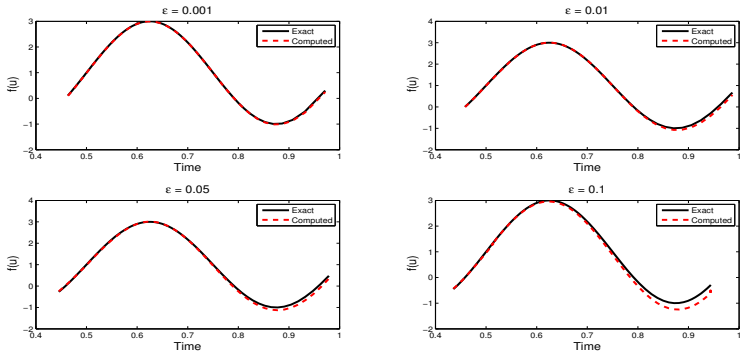

Figure 5: The exact and numerical approximations of $f(u)$ in Example 1 when $\alpha = 0.5$.

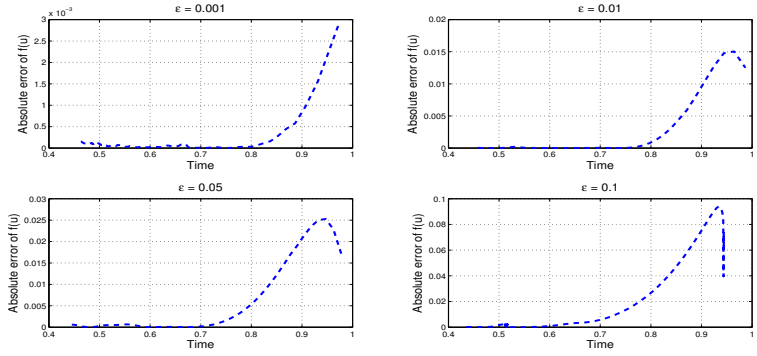

Figure 6: Absolute error of numerical approximations $f(u)$ in Example 1 when $\alpha = 0.5$.

Table 1: The relative weighted l_2-norm errors between the computed and the exact values of $u(1,t)$, $u_x(1,t)$ and $f(u)$ in Example 1 for various values of h, k and ε.

		$\alpha = 0.25$			$\alpha = 0.75$		
N	M	$\sigma_N(u)$	$\sigma_N(u_x)$	$\sigma_N(f)$	$\sigma_N(u)$	$\sigma_N(u_x)$	$\sigma_N(f)$
$\varepsilon = 0.01$							
50	64	0.0032	0.0057	0.0288	0.0171	0.0299	0.0356
50	128	0.0028	0.0046	0.0235	0.0109	0.0206	0.0283
50	256	0.0022	0.0035	0.0186	0.0087	0.0153	0.0229
100	64	0.0027	0.0049	0.0253	0.0152	0.0261	0.0311
100	128	0.0023	0.0042	0.0202	0.0093	0.0182	0.0241
100	256	0.0018	0.0031	0.0173	0.0071	0.0105	0.0185
$\varepsilon = 0.05$							
50	64	0.0093	0.0239	0.0456	0.0285	0.0403	0.0517
50	128	0.0085	0.0187	0.0377	0.0162	0.0325	0.0473
50	256	0.0070	0.0133	0.0290	0.0111	0.0292	0.0411
100	64	0.0090	0.0215	0.0411	0.0263	0.0373	0.0496
100	128	0.0078	0.0160	0.0356	0.0120	0.0306	0.0432
100	256	0.0062	0.0117	0.0266	0.0098	0.0257	0.0361
$\varepsilon = 0.1$							
50	64	0.0225	0.0513	0.0637	0.0399	0.0566	0.0770
50	128	0.0191	0.0422	0.0576	0.0325	0.0511	0.0692
50	256	0.0150	0.0385	0.0469	0.0271	0.0436	0.0618
100	64	0.0203	0.0493	0.0592	0.0362	0.0516	0.0713
100	128	0.0174	0.0401	0.0511	0.0270	0.0455	0.0652
100	256	0.0122	0.0362	0.0443	0.0211	0.0372	0.0600

6 Conclusion

In this article, a numerical algorithm for solving an inverse problem of a time-fractional inverse heat conduction equation with an unknown nonlinear boundary function is proposed. According to the ill-posedness of the problem, first the mollification regularization method is applied. Afterwards, a marching finite difference scheme is used to solve the stabilized problem. Stability and convergence analysis are theoretically proven. Finally, two numerical examples are provided to demonstrate the stability and convergence behaviours of the presented method.

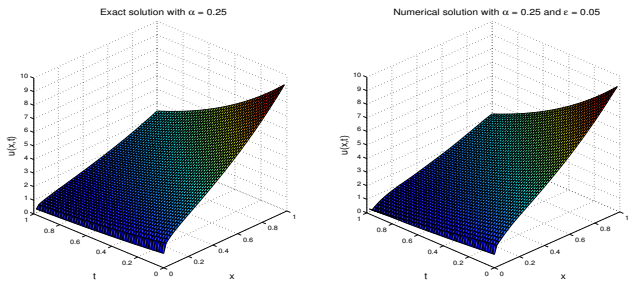

Figure 7: The exact and numerical solutions of $u(x,t)$ for Example 2 when $\alpha = 0.25$ and $\varepsilon = 0.05$.

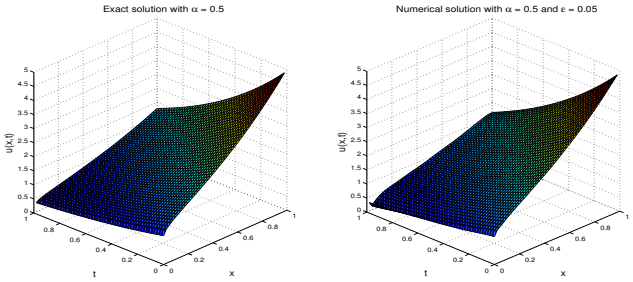

Figure 8: The exact and numerical solutions of $u(x,t)$ for Example 2 when $\alpha = 0.5$ and $\varepsilon = 0.05$.

References

[1] T.J. Anastasio, *The fractional-order dynamics of brainstem vestibulo-oculomotor neurons*, Biol. Cybern. **72** (1994) 69–79.

[2] A. Babaei and S. Banihashemi, *A Stable Numerical Approach to Solve a Time-Fractional Inverse Heat Conduction Problem*, Iran J. Sci. Technol. Trans. Sci. **42**(4) (2017) 2225-2236.

[3] D. Baleanu, J.A. Tenreiro Machado and A.C.J. Luo, *Fractional Dynamics and Control*, Springer, New York, 2012.

[4] A. Dabiri, B.P. Moghaddam and J.A. Tenreiro Machado, *Optimal variable-order fractional PID controllers for dynamical systems*, J. Comput. Appl. Math. **339** (2018) 40–48.

Table 2: The relative weighted l_2-norm errors between the computed and the exact values of $u(1,t)$, $u_x(1,t)$ and $f(u)$ in Example 2 for various values of h, k and ε.

		$\alpha = 0.3$			$\alpha = 0.6$		
N	M	$\sigma_N(u)$	$\sigma_N(u_x)$	$\sigma_N(f)$	$\sigma_N(u)$	$\sigma_N(u_x)$	$\sigma_N(f)$
$\varepsilon = 0.01$							
50	64	0.0017	0.0263	0.0046	0.0017	0.0477	0.0384
50	128	0.0013	0.0185	0.0033	0.0015	0.0336	0.0365
50	256	0.0009	0.0130	0.0021	0.0011	0.0237	0.0326
100	64	0.0018	0.0243	0.0038	0.0014	0.0467	0.0356
100	128	0.0011	0.0152	0.0030	0.0012	0.0312	0.0325
100	256	0.0006	0.0111	0.0026	0.0009	0.0219	0.0290
$\varepsilon = 0.05$							
50	64	0.0049	0.0266	0.0162	0.0055	0.0522	0.0505
50	128	0.0045	0.0193	0.0154	0.0042	0.0460	0.0435
50	256	0.0033	0.0139	0.0127	0.0036	0.0411	0.0382
100	64	0.0047	0.0249	0.0150	0.0050	0.0486	0.0416
100	128	0.0036	0.0171	0.0110	0.0039	0.0425	0.0363
100	256	0.0031	0.0133	0.0101	0.0033	0.0376	0.0302
$\varepsilon = 0.1$							
50	64	0.0086	0.0372	0.0203	0.0078	0.0589	0.0796
50	128	0.0065	0.0265	0.0139	0.0062	0.0500	0.0660
50	256	0.0052	0.0211	0.0122	0.0053	0.0433	0.0575
100	64	0.0080	0.0321	0.0158	0.0073	0.0532	0.0711
100	128	0.0063	0.0240	0.0120	0.0060	0.0481	0.0631
100	256	0.0044	0.0199	0.0100	0.0048	0.0411	0.0560

[5] Y. Ding, Z. Wang and H. Ye, *Optimal control of a fractional-order HIV-immune system with memory*, IEEE Trans. Control Syst. Technol. **20**(3) (2012) 763–769.

[6] S. Fomin, V. Chugunov and T. Hashida, *Application of fractional differential equations for modeling the anomalous diffusion of contaminant from fracture into porous rock matrix with bordering alteration zone*, Trans. Porous Med. **81** (2010) 187–205.

[7] M. Garshasbi and H. Dastour, *A mollified marching solution of an inverse ablation-type moving boundary problem*, Comput. Appl. Math. **35** (2016) 61–73.

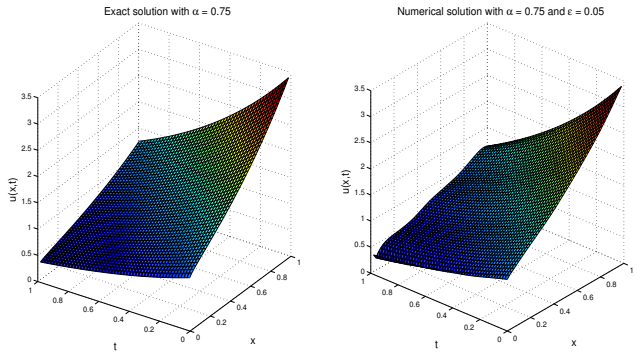

Figure 9: The exact and numerical solutions of $u(x,t)$ for Example 2 when $\alpha = 0.75$ and $\varepsilon = 0.05$.

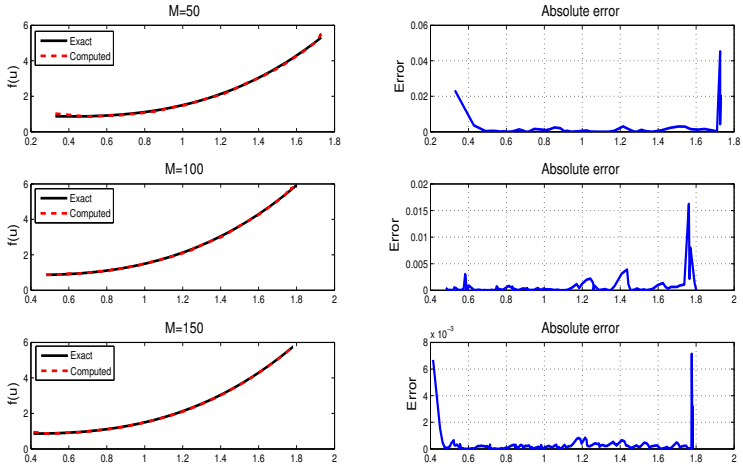

Figure 10: The exact and numerical solutions (left) and absolute error (rigth) of $f(u)$ for Example 2 when $\alpha = 0.5$ and $\varepsilon = 0.01$.

[8] D.N. Hao, *A mollification method for ill-posed problems*, Numer. Math. **68** (1994) 469–506.

[9] H. Jafari, *Numerical solution of time-fractional Klein-Gordon equation by Using the decomposition methods*, J. Comput. Nonlinear Dyn. **11** (4) (2016) 041015.

[10] B. Jin and W. Rundell, *A tutorial on inverse problems for anomalous diffusion processes*, Inverse Probl. **31** (2015).

[11] M. Kirane and S. A. Malik, *Determination of an unknown source term and the temperature distribution for the linear heat equation involving fractional derivative in time*, Appl. Math. Comput. **218** (2011) 163–170.

[12] R. Metzler and J. Klafter, *The random walk's guide to anomalous diffusion: A fractional dynamics approach*, Phys. Rep. **339** (2000) 1–77.

[13] D. A. Murio, *Mollification and space marching, in: K. Woodbury (Ed.), Inverse Engineering Handbook*, CRC Press, Boca Raton FL, 2002.

[14] D.A. Murio, *On the stable numerical evaluation of Caputo fractional derivatives*, Comput. Math. Appl. **51** (2006) 1539–1550.

[15] D. A. Murio and C.E. Mejia, *Generalized time fractional IHCP with Caputo fractional derivatives*, J. Phys: Conference Series **135** (2008) 1–8.

[16] K.B. Oldham and J. Spanier, *The Fractional Calculus: Theory and Application of Differentiation and Integration to Arbitrary Order*, Academic Press, New York, 1974.

[17] G. Ozkum, A. Demir, S. Erman, E. Korkmaz and B. Ozgur, *On the inverse problem of the fractional heat-like partial differential equations: determination of the source function*, Adv. Math. Phys., 2013, Article ID 476154.

[18] I. Podlubny, *Fractional Differential Equations*, Academic Press, New York, 1999.

[19] R. Pourgholi, A. Esfahani and M. Abtahi, *A numerical solution of a two-dimensional IHCP*, J. Appl. Math. Comput. **41** (2013) 61–79.

[20] Z. Qian, *Optimal modified method for a fractional-diffusion inverse heat conduction problem*, Inverse Probl. Sci. Eng. **18** (2010) 521–533.

[21] W. Rundell, X. Xu and L. Zuo, *The determination of an unknown boundary condition in a fractional diffusion equation*, Appl. Anal. **92** (2013) 1511–1526.

[22] E. Scalas, R. Gorenflo and F. Mainardi, *Fractional calculus and continuous-time finance*, Physica A **284** (2000) 376–384.

[23] R. Schumer, D. Benson, M. Meerschaert and S. Wheatcraft, *Eulerian derivation of the fractional advection-dispersion equation*, J. Contam. Hydrol. **48** (2001) 69–88.

[24] R. Schumer, M. Meerschaert and B. Baeumer, *Fractional advection-dispersion equations for modeling transport at the earth surface*, J. Geophys. Res. Earth Surf. **114** (2009).

[25] R.T. Sibatov and V.V. Uchaikin, *Dispersive transport of charge carriers in disordered nanostructured materials*, J. Comput. Phys. **293** (2015) 409–426.

[26] A. Taghavi, A. Babaei and A. *Mohammadpour, A stable numerical scheme for a time fractional inverse parabolic equation*, Inverse Probl. Sci. Eng. **25**(10) (2017) 1474–1491.

[27] C. Wang, L. Ling, X. Xiong and M. Li, *Regularization for 2-D fractional sideways heat equations*, Numer. Heat Tr. B-Fund. **68** (2015) 418–433.

[28] M. Q. Wang, C. X. Wang, M. Li and C. S. Chen, *A numerical scheme based on FD-RBF to solve fractional-diffusion inverse heat conduction problems*, Numer. Heat Tr. A-Appl. **68** (2015) 978–992.

[29] X.T. Xiong, J.X. Wang and M. Li, *An optimal method for fractional heat conduction problem backward in time*, Appl. Anal. **91** (2012) 823–840.

[30] F. Yang, C.L. Fu and X.X. Li, *A mollification regularization method for unknown source in time-fractional diffusion equation*, Intern. J. Computer Math. **91**(7) (2014) 1516–1534.

[31] J. Zhang and K. Chen, *Variational image registration by a total fractional-order variation model*, J. Comput. Phys. **293** (2015) 442–461.

[32] Q. Zhuang, B. Yu and X. Jiang, *An inverse problem of parameter estimation for time fractional heat conduction in a composite medium using carbon-carbon experimental data*, Physica B: Condens. Matter. **456** (2015) 9–15.